MODELING THE RISK OF FIRE/EXPLOSION DUE TO OXIDIZER/FUEL LEAKS IN THE ARES I INTERSTAGE

Robert Ring[(1)], James Stott[(2)], Christy Hales[(3)]

[(1)]Bastion Technologies, Inc., MSFC, AL 35812, USA, Email: robert.w.ring@nasa.gov
[(2)]NASA/MSFC, QD 33, MSFC, AL 35812, USA , Email: james.e.stott@nasa.gov
[(3)]Bastion Technologies, Inc, MSFC, AL 35812, USA, Email: christy.a.hales@nasa.gov

ABSTRACT

A significant flight hazard associated with liquid propellants, such as those used in the upper stage of NASA's new Ares I launch vehicle, is the possibility of leakage of hazardous fluids resulting in a catastrophic fire/explosion. The enclosed and vented interstage of the Ares I contains numerous oxidizer and fuel supply lines as well as ignition sources. The potential for fire/explosion due to leaks during ascent depends on the relative concentrations of hazardous and inert fluids within the interstage along with other variables such as pressure, temperature, leak rates, and fluid outgasing rates. This analysis improves on previous NASA Probabilistic Risk Assessment (PRA) estimates of the probability of deflagration, in which many of the variables pertinent to the problem were not explicitly modeled as a function of time. This paper presents the modeling methodology developed to analyze these risks.

1. MOTIVATION

NASA's Marshall Space Flight Center is currently developing hardware and systems for the Ares I rocket that will send future astronauts into orbit. Built on cutting-edge launch technologies, evolved powerful Apollo and Space Shuttle propulsion elements, and decades of NASA spaceflight experience, Ares I is the essential core of a safe, reliable, cost-effective space transportation system. The development of safe and reliable launch vehicles is vitally important to Ares I mission success. Probabilistic modeling and simulation of phenomenological events is an important component of the Ares I Upper Stage Element PRA.

A significant flight hazard associated with liquid rockets is the possibility of leakage of hazardous fluids, such as liquid oxygen and hydrogen, resulting in a catastrophic fire/explosion. A primary function of the Ares I Upper Stage Main Propulsion System is to supply stored propellants to the J-2X Upper Stage Engine (USE). The enclosed and vented interstage contains numerous oxidizer and fuel supply lines as well as ignition sources. The potential for fire/explosion due to leaks during ascent depends on the relative concentrations of hazardous and inert fluids within the interstage along with other variables such as pressure, temperature, leak rates, and fluid outgasing rates. This dynamic environment must be modeled in order to obtain credible estimates of the probability of deflagration for a range of credible leakage scenarios. This analysis improves upon the methodology used in the Space Shuttle PRA, which did not explicitly model many of the time-dependent variables that are pertinent to the problem.

2. PURPOSE AND SCOPE

2.1. Purpose

The purpose of this paper is to explain the modeling methodology used to estimate the risk of fire or explosion due to hydrogen and oxygen leaks in the Ares I interstage for the NASA Ares I Upper Stage Element PRA. It also provides information on how various relevant data were collected and a description of the output from the model.

2.2. Scope

The scope of this study is the Ares I Design Analysis Cycle 2A (DAC-2A) configuration. The region of the vehicle considered is the enclosed volume of the aft skirt, interstage, and forward frustum, and the enclosed volume of the thrust cone. The timeline of analysis begins at liftoff and ends at first stage separation. Leakages from the Main Propulsion System (MPS) and USE are considered. The primary scenarios considered pertain to hydrogen and oxygen leaks. Secondarily, we considered scenarios involving air incursion.

3. INTERSTAGE DESIGN

3.1. Configuration Overview

The interstage region is defined as the region consisting of the aft skirt, the interstage, and the forward frustum. The interstage is the primary structural interface between the Ares I first stage and upper stage, and it encloses the thrust cone and USE. The interstage is

attached to the aft skirt of the upper stage at one end, and the forward frustum at the other end. The primary function of the frustum is to interface between the smaller diameter first stage and the larger diameter upper stage. The forward frustum attaches to the first stage forward skirt extension. The structure at the top of the first stage forward skirt extension is the aeroshell. The aeroshell protects the drogue and pilot parachutes during flight and reentry. The layout shown in Figure 1 depicts the region described.

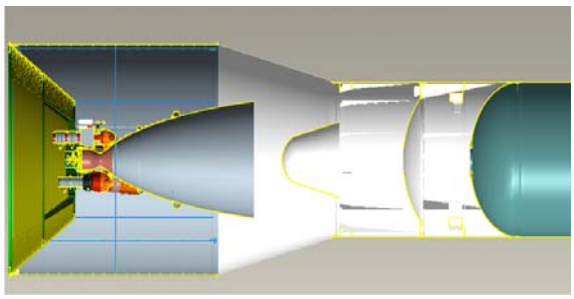

Figure 1. DAC-2 schematic of interstage region

3.2. Volume of Interstage Enclosure

The volume of the interstage was estimated from design schematics and by assuming the interstage is made up of two perfect cylinders and one frustum, and then subtracting out the volumes of a cone representing the USE, a cone representing the aeroshell, and a portion of a sphere representing the oxygen tank. An additional percentage of the total was subtracted to allow for displacement of volume by various structures found in the interstage.

4. FLAMMABILITY CRITERIA [1]

4.1. Hydrogen Flammability Limits

Flammability of hydrogen occurs between specific limits. These limits are a function of temperature, pressure, diluents, and ignition energy. Concentration limits are normally expressed as percent by volume (%v/v). For hydrogen in an air mixture, the Lower Flammability Limit (LFL) and Upper Flammability Limit (UFL) are 4% and 75%, respectively. In oxygen, the limits are 4% and 94%, respectively.

4.2. Effect of Diluents on Flammability Limits

A flammability diagram representing the flammability limits for hydrogen in the diluent nitrogen at Standard Ambient Temperature and Pressure (SATP) is shown in Fig. 2. The region inside the red line represents the flammability region for different concentrations of hydrogen, oxygen, and nitrogen. Outside the red line, hydrogen gas is not flammable.

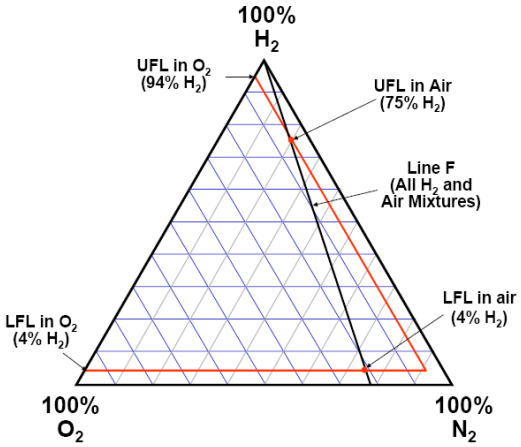

Figure 2 Flammability diagram for hydrogen in nitrogen at SATP

4.3. Effect of Temperature on Flammability Limits

In general, at constant pressure, the flammability range of hydrogen expands as temperature increases and narrows as the temperature decreases. Fig. 3 shows that when temperature increases at constant standard pressure, the LFL decreases.

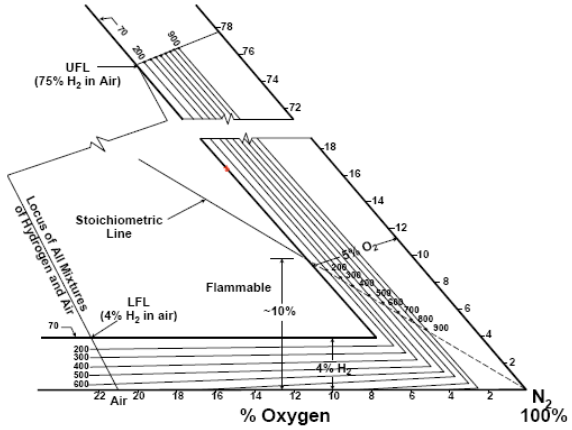

Figure 3. Effects of temperature on the flammability range of hydrogen

4.4. Effect of Pressure on Flammability Limits

Similar to temperature, the flammability range of the gas expands as pressure increases and narrows as the pressure decreases at constant temperature. This is apparent since temperature and pressure are also positively correlated. The effects of reduced pressure on hydrogen flammability in air at standard ambient temperature are shown in Tab. 1.

Table 1. Effects of reduced pressure at standard ambient temperature

Conditions	Hydrogen Content vol%			
	Upper propagation		Downward propagation	
Hydrogen in air at reduced pressure with a 45 mJ (47.5 Btu) ignition source:				
Pressure kPa	25 cm Tube		2 L Sphere	
	Lower limit	Upper limit	Lower limit	Upper limit
20	≈ 4	≈ 56	≈ 5	≈ 52
10	≈ 10	≈ 42	≈ 11	≈ 35
7	≈ 15	≈ 33	≈ 16	≈ 27
6	20-30		20-25 (at 6.5 kPa)	

4.5. Ignition Energy and Relation to Flammability Limits

Tab. 2 shows pressure effects on the minimum ignition energy required to cause combustion of hydrogen in air given the hydrogen concentration is within the flammability limits. It can be seen that the minimum ignition energy increases as the pressure decreases. It should also be noted that an electrostatic discharge, i.e. shock when touching a doorknob after walking across carpet, is normally much greater than the lowest minimum ignition energy for hydrogen.

Table 2. Pressure effects on hydrogen minimum ignition energy

Ignition Energy	Pressure	Pressure
(mJ)	(kPa)	(psia)
0.017	101.3	14.7
0.09	5.1	0.735
0.56	2.03	0.294

4.6. Limiting Oxygen Index

The Limiting Oxygen Index (LOI) is the minimum concentration of oxygen that will support flame propagation in a mixture of hydrogen, air, and nitrogen. A conservative estimate of the LOI can be found in Eq. 1, where z is the stoichiometric amount of oxygen required in the combustion reaction.

$$LOI \cong z \cdot LFL \tag{1}$$

For example, the combustion reaction for hydrogen is shown in Eq. 2.

$$2H_2 + O_2 \longrightarrow 2H_2O + \Delta H_c \tag{2}$$

For, this reaction, the heat of combustion, ΔH_c, is 68.1 kcal/mol. We see in this equation that we require 1 mole of oxygen to 2 moles of hydrogen for the reaction to occur. In this case, z = 1. We further know from Tab. 1 that the LFL of hydrogen is approximately 4%. Thus, we have Eq. 3.

$$LOI \cong z \cdot LFL = 4\% \tag{3}$$

We know experimentally that the true LOI for hydrogen is approximately 5%. Thus, we have a conservative estimate for the LOI of hydrogen at SATP.

5. ATMOSPHERIC TEMPERATURE, PRESSURE, AND ALTITUDE

Atmospheric pressure and temperature are positively correlated quantities.

The temperature of the Earth's atmosphere varies with altitude, and the mathematical relationship between temperature and altitude varies between the different atmospheric layers.

Atmospheric pressure is a direct result of the total weight of the air above the point at which the pressure is measured. This means that air pressure varies with location and time because the amount (and weight) of air above the earth varies with location and time.

Atmospheric pressure decreases with height, dropping by 50% at an altitude of about 5.6 km (~185 kft). This pressure drop is approximately exponential, so that each doubling in altitude results in an approximate decrease in pressure by half. However, because of changes in temperature throughout the atmospheric column as well as the fact that the force of gravity begins to decrease at great altitudes, a single equation does not model atmospheric pressure through all altitudes. Like temperature, it is modeled differently in each of the atmospheric layers. Fig. 4 notionally shows how temperature and pressure vary with altitude.

The model uses temperature and pressure data taken from the Program's Natural Environment Definition for Design. These data are expressed as mean temperature and pressure along with standard deviations for various altitudes above the Eastern Test Range.

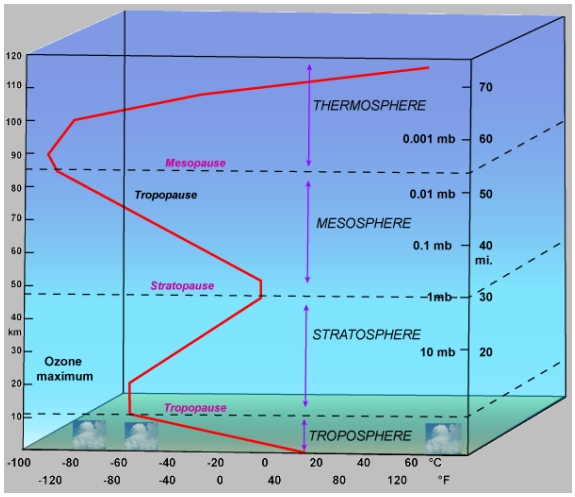

Figure 4. Variation of temperature and pressure in the atmosphere

6. IDEAL GAS LAW

The ideal gas law is the equation of state of a hypothetical ideal gas. The amount of gas n (mol) contained in a volume V (ft^3) is determined by its pressure P (psia) and temperature T (K). The relationship is given in Eq. 4.

$$PV = nRT \tag{4}$$

The constant R = 0.0426 (psia ft^3 / mol K) is the ideal gas constant.

The ideal gas law is most accurate for monatomic gases. The approximation breaks down at high pressures and low temperatures, where the intermolecular forces play a greater role in determining the properties of the gas. It does not factor in the size of each gas molecule or the effects of intermolecular attraction.

7. GROUNDRULES AND ASSUMPTIONS

Initial concentrations of hydrogen, oxygen, and nitrogen are based on ground operations analyses. During cryo loading from several hours prior to launch until liftoff, a nitrogen purge is continuously applied to the interstage, which prevents accumulation of hazardous gas leakage. At T-0 the nitrogen purge is terminated and a helium purge begins entering the engine and continues throughout the ascent phase. A small additional amount of helium, not considered in the model, comes from a helium driven turbine pump. A positive differential pressure results in outgasing of nitrogen from liftoff to first stage separation. Therefore, in order to achieve the necessary threshold concentrations of hydrogen and oxygen enabling deflagration, only those scenarios that envisage both hydrogen and oxygen sources are considered credible. While the presence of hydrogen implies a leak source, oxygen may enter the system from leak sources or from incursion of air. In this study, all leak sources of either fluid type are assumed to begin at T-0 and continue at a constant rate throughout ascent.

The rate of outgasing is determined by nulling the pressure differential at the end of each simulation time step throughout ascent.

The threshold leak sizes required to produce deflagration depend upon the LFL, UFL, and LOI. These limits are assumed to be based solely on the concentration of the gases and pressure since they are the most significant factors during ascent. Their values are interpolated from data tables at each time step.

Deflagration occurs whenever the concentration of hydrogen and oxygen accumulate to within the flammability limits and an ignition source of sufficient energy is present. Because numerous energetic sources exist in the interstage, an ignition source is assumed.

For scenarios in which both oxygen and hydrogen are leaking, we assumed that no air incursion occurs; thus, the only source of oxygen is from leaks and the only source of nitrogen is the initial purge.

Mixing of gases within the reference volumes is not well understood; therefore, we separately analyzed two sets of results: 1) by assuming perfect instantaneous mixing, and 2) by using a conservative assumption in which all nitrogen is assumed to leave the interstage before the hydrogen, oxygen, and helium. Assumption 2) was used to produce the result shown in this paper. (6.1)

8. METHODOLOGY

The model uses a Monte Carlo simulation to sample randomly from various potential flight profiles. Each of 50,000 iterations per model run begins at T-0 and continues until first stage separation. For each iteration, the altitude is obtained from the trajectory table and then temperature is sampled from a normal distribution based on the mean and standard deviation values from the Eastern Test Range atmospheric data table, which is correlated to ground conditions at time of launch. Atmospheric pressure is correlated to the sampled temperature via the standard atmosphere model and the ideal gas law. The concentrations of hydrogen, oxygen, nitrogen, and helium within the interstage are then updated using the pressure differential, current temperature, moles of gas entering since the last update time, and the ideal gas law.

The nominal ascent trajectories (altitude vs. time) used in this study were based on launching from Kennedy Space Center to support the International Space Station.

8.1. Distribution of Leak Sizes

Estimates of leak size for specific scenarios of interest depend largely on expert elicitations with subject matter experts. Whenever historical data is available, such as experience from the Space Shuttle, statistical data analysis methods are used to fit a distribution to the data. The data from the Space Shuttle Main Propulsion System Feedline Interface Seal (F1) at the hydrogen inlet and the (O1) seal at the oxygen inlet are good examples. These are a Teflon-coated, thin-lipped design shown in Fig. 5. The leak check used helium at 25 psig with the leakage being measured through a vent port connected to a Rota meter flow meter.

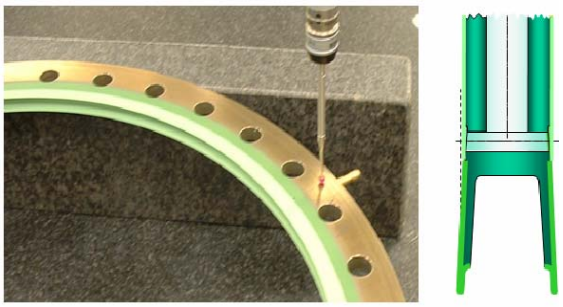

Figure 5. SSME F1/O1 Feedline Seal

The seals are fixed, feedline seals similar in design to the feedline seals expected to be used in the Ares I Upper Stage MPS. Because of their location on the Shuttle, these seals experience a more severe flight environment than would be seen on Ares I. The standardized skewness of the data indicates a highly right-skewed distribution. Fig. 6 shows a histogram plot of the data.

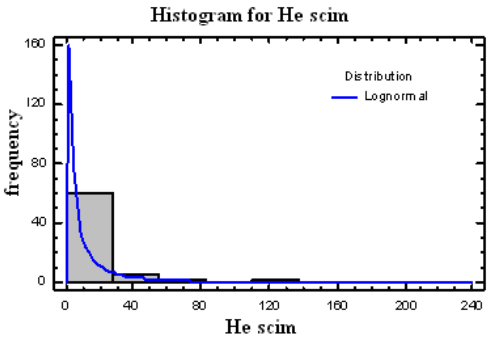

Figure 6. Histogram/lognormal fit: SSME O1/F1 interface helium leak data

Previous analyses indicated the use of the lognormal distribution to represent the leak size distribution [2]. Fig. 7 is a quantile-quantile plot of the data. The data is adequately modeled by the lognormal when it plots approximately as a straight line. Evidence of lack of fit in the right tail is more important than in the body or the left tail. There appears to be a good fit in the body and right tail of the data to the model; therefore, in this case we conclude that the data is adequately modeled by the lognormal distribution.

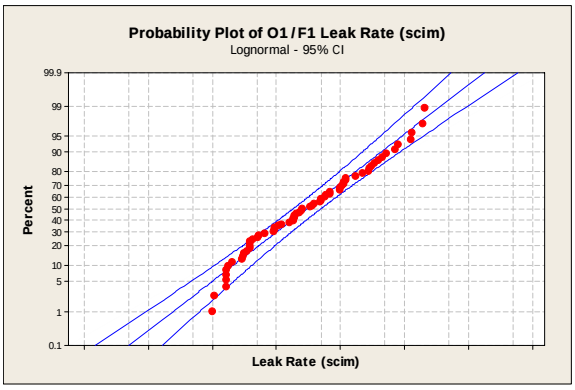

Figure 7. Quantile–quantile plot: SSME O1/F1 interface

Because the leak checks were conducted using helium gas, we must estimate the leak size for hydrogen and oxygen. The leak rate conversion factor from helium to hydrogen and oxygen is based on the ratio of molecular weights [3].

8.2. Probability of Leak Occurrence

The Fault Risk Analysis Spreadsheet (FRAS) is a tool developed for earlier work on nuclear power plant PRAs [4]. It has been used for predicting the probabilities for critical events of a phenomenological nature (leaks, debonding of thermal protection coatings, ruptures, etc.) when applicable historical data are available.

FRAS estimates defect occurrence frequency and defect size in a flight mission from raw, historical defect data derived from flight experience and from test and inspection discrepancy reports. The raw data is modified by applying analyst's effectiveness factors for corrective actions, such as design modification, tests and inspections, and other hazard controls. The resultant estimate of the mean defect size determines a distribution of defect sizes experienced in a mission. FRAS has also been used to estimate the frequency of random independent leaks in flight by using the methods described above. FRAS is not applicable to estimating dependent leak events.

9. SAMPLE RESULTS

After the Monte Carlo simulation is completed, the stored sampling data are used to develop probability distributions for the concentrations of hydrogen, oxygen, nitrogen, and helium within the interstage as a function of time. Recall that deflagration occurs whenever the concentrations of hydrogen and oxygen are jointly within their lower and upper limits. Direct estimation of the probability of deflagration from the sampling data is not feasible because the frequency is too low. Instead we use the sampling distributions for the concentrations of hydrogen and oxygen at each time to calculate the joint probabilities of being within the deflagration limits. In other words, deflagration occurs when the events described in Eq. 5 both occur.

$$X(t) \geq LOI(t) \text{ and } LFL(t) \leq Y(t) \leq UFL(t) \quad (5)$$

Where X(t) is the sampling distribution for oxygen concentration at time t and Y(t) is the sampling distribution for hydrogen concentration at time t. The probabilities of each of these events are calculated from the lower and upper tail probabilities. The mission probability of deflagration *P* is calculated from the *N* time step probabilities *p(i)* as

$$P = 1 - \prod_{i=1}^{N} (1 - p(i)) . \quad (6)$$

This process is carried out for a variety of hydrogen and oxygen leak rates, and the results are then compiled into a contour map based on initial leak rates, so that given any total leak rate for hydrogen and oxygen, a probability of deflagration may be ascertained. These data may than be used to assess the probability of deflagration associated with specific leakage scenarios.

The results of all the model runs are compiled in Fig. 8. All points in the blue field of the Fig. 8 indicate a probability of deflagration beyond the detection ability of the model, or less than about 10^{-30}.

The contour plot shows that an oxygen leak rate of about Y and a hydrogen leak rate of about X are required to get a probability of deflagration of 1. (Note that at this point, the log of probability of deflagration is 0.) The current combined allowable hydrogen leakage limit for the USE and MPS is slightly greater than x. Although, this is great enough to cause some concern, the current allowable leakage limit for oxygen is substantially below y. As long as the total oxygen leakage does not exceed y, the risk of deflagration is not credible.

10. SENSITIVITY ANALYSES PERFORMED (0.1)

10.1. Ideal Gas Law Assumption

A comparison of the ideal gas law and the more accurate Van der Waal's equation of state found results agree to within 0.1%. By the time of greatest interest in the model, the percent difference is even lower. Therefore, the simpler idea gas law is used in the model.

10.2. Mixing Assumption

As previously mentioned, two sets of results were run to determine the affects of mixing within the interstage. In addition to the model runs assuming the nitrogen exits the interstage before the hydrogen, oxygen, and helium, analyses were also conducted assuming perfect, instantaneous mixing of the gases as well as several variations that fall between no mixing and perfect mixing. The assumption that nitrogen leaves first is conservative. Further investigation into the local variation in hydrogen and oxygen concentrations is being pursued in a related study using computational fluid dynamics.

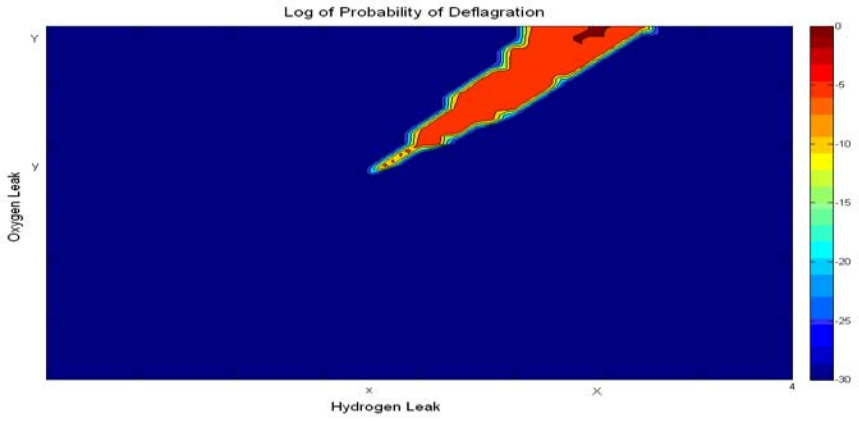

Figure 8. Log of probability of deflagration as a function of leak size

10.3. Air Incursion Scenarios

Scenarios involving hydrogen leaks plus air incursion were addressed as a sensitivity. Incursion rates of up to 35,000 scim were examined. The model indicated that air incursion as the oxygen source up to the levels analyzed, does not enable deflagration. This is because air is about 21% oxygen and by the time the model suggests deflagration could occur, the LOI is significantly greater than 21%. Consequently, the relative importance of scenarios involving air incursion as the main oxygen source has been downgraded.

10.4. Venting Assumption

Pressure profiles from a variety of venting scenarios for various flight trajectories were used in some analyses rather than assuming the interior pressure equaled the atmospheric pressure. In all cases, the pressure lag induced by using a realistic venting scenario decreased the probability of deflagration since nitrogen did not leave the interstage volume as rapidly. Even in cases where perfect instantaneous mixing was assumed, the instantaneous equilibration of pressure provided higher probabilities of deflagration than using a more realistic model for pressure. In these cases, the analysis was strictly deterministic as not enough data is currently available on venting to perform a proper Monte Carlo analysis.

10.5. Modeling Dependent Leaks

The total leak size is the key factor contributing to the probability of deflagration. The total leak size consists of nominal leakage plus leakage due to abnormal challenges to the system. Multiple leaks may result from common susceptibility to a challenge. Additionally, the sizes of multiple leaks are likely to be positively correlated. Positively correlated leaks pose a greater risk of deflagration than uncorrelated leaks. To illustrate, consider m hydrogen feedline seal leaks. Assume the total leak rate is the sum of m identically distributed random variables. The correlation coefficient can range from 0 for uncorrelated to 1 for perfectly correlation.

We consider these bounding cases, which are illustrated in Fig. 9. In this example, we summed m=10 identically distributed lognormal variables (mean=1,000 scim, error factor=5). (The error factor is a measure of dispersion equal to the 95th percentile divided by the median.) The unshaded curve is the sum of uncorrelated variables while the shaded curve represents the sum of perfectly correlated variables. The mean of the sum is 10,000 scim in either case; but, the dispersion is much larger for the correlated sum.

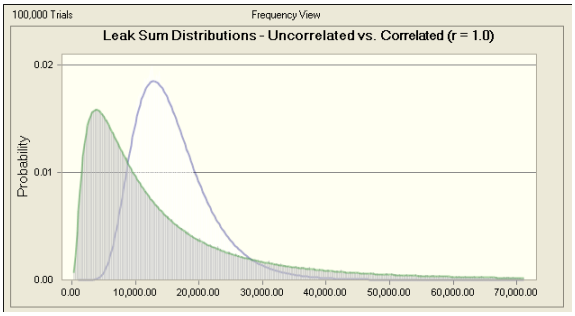

Figure 9. Perfectly Correlated vs. Uncorrelated Leak Sum Distributions

Assuming the ambient oxygen in the interstage is the maximum allowable, it required 4 perfectly correlated oxygen leaks for a significant increase in probability of deflagration versus more than 10 uncorrelated oxygen leaks. In these cases, hydrogen leak rates were assumed to be at a worse case level.

This illustrates the importance of estimating the degree of correlation whenever multiple leaks due to a common system challenge are considered. Structured expert elicitation methods may be helpful in this regard [5]. These methods are being pursued as forward work.

11. SUMMARY AND CONCLUSIONS

This model allows NASA to estimate the risk of deflagration due to hazardous fluid leakage by modeling the dynamic flight environment. Instead of using a broad system-level approach to arrive at an estimate, the most pertinent information is taken into account and changes in atmosphere and flammability are examined as a function of time. This model also has the benefit of being able to accommodate a variety of different specific failure scenarios.

S&MA is responding to requests from NASA's engineering directorate to help them assess the impact of design changes on leakage allowables. This model is uniquely capable of comparing risks of deflagration associated with various potential designs, allowing quantitative risk measurements to guide the design of Ares I.

This model is being employed to support phenomenological risk modeling within the Ares I Upper Stage PRA. The focus of this effort is to work within the integrated design teams to identify risk drivers and to influence design for improved safety and reliability. As the PRA is updated to support all phases of the program lifecycle, the model will continue to evolve.

12. REFERENCES

1 ANSI/AIAA G-095-2004. (2004). *Guide to Safety of Hydrogen and Hydrogen Systems*.

2 Ring, R.W. (2004). External Tank (ET) Leak Data Analysis, Presentation to the Shuttle PRA Independent Peer Review Panel, Rockville, M.D.

3 Grout, P.A. (2001). Improvement of Hydrazine-He Leak Limit by Comparing Liquid-Gas Leak Data to Theoretical Leak Correlation, Graduate Research Project Submitted to Embry-Riddle Aeronautical University.

4 Vesely, W.E. (2003). The Treatment of Fault Criticality Potential in FRAS.

5 Kurowicka, D. and Cooke, R. (2006). *Uncertainty Analysis with High Dimensional Dependence Modelling,* John Wiley, Ltd. West Essex, England.